Materials Today: Proceedings xxx (xxxx) xxx

Contents lists available at ScienceDirect

Materials Today: Proceedings

journal homepage: www.elsevier.com/locate/matpr

A study of electron regeneration efficiency in fluorophore

N.F. Shaafi [a], S.B. Aziz [b,c], M.F.Z. Kadird [d], S.K. Muzakir [a,*]

[a] Material Technology Programme, Faculty of Industrial Sciences and Technology, Universiti Malaysia Pahang, Lebuhraya Tun Razak, Gambang 26300 Kuantan, Pahang, Malaysia
[b] Advanced Polymeric Materials Research Lab., Department of Physics, College of Science, University of Sulaimani, Qylasan Street, Sulaimani, Kurdistan Regional Government-Iraq, Iraq
[c] Department of Civil Engineering, College of Engineering, Komar University of Science and Technology, Sulaimani 46001, Kurdistan Regional Government, Iraq
[d] Center of Foundation Studies in Science, University of Malaya, 50603 Kuala Lumpur, Malaysia

ARTICLE INFO

Article history:
Available online xxxx

Keywords:
Efficient electron regeneration
CMC/PVA
Alginate
Redox potential
DFT

ABSTRACT

Archetypical excitonic solar cell consists of fluorophore (main light absorber), photoelectrode (electron transportation), and conducting polymer (electron regeneration). Fluorophore generates excited state electron upon absorption of light with sufficient energy. Electron in the highest occupied molecular orbitals (HOMO) would undergo an excitation to the lowest unoccupied molecular orbitals (LUMO) during the light absorption process. Therefore an electron vacancy in the HOMO of fluorophore is expected; need to be replenished for a continuous process of a photovoltaic mechanism. However the quantum of research on electron regeneration efficiency is still low due to limited computational facility. Two parameters are hypothesized to have significant impact on the electron regeneration process i.e., (i) conductivity (σ), and (ii) redox potential (E^o) of the conducting polymer. This study aims to establish a correlation between the stated parameters with the photovoltaic conversion efficiency, η. Two conducting polymer were used in this work i.e., (i) alginate, and (ii) a mixture of 60 wt% of carboxymethyl cellulose (CMC) and 40 wt% of polyvinyl alcohol (PVA). The conductivity of the conducting polymer was calculated based on the measured bulk resistance using Electrical Impedance Spectrometer (EIS); showed that $\sigma_{alginate} > \sigma_{CMC/PVA}$. The redox potentials were calculated using quantum chemical calculations under the framework of density functional theory (DFT) at the level of b3lyp/lanl2dz. The lead sulphide thin film (fluorophore) was deposited using thermal evaporator on a pre-fabricated TiO_2 layer on indium-doped tin oxide (ITO) conducting glass. The CMC/PVA-based cell yielded the highest η of 0.0015% under one-sun condition; showed higher η than that of the alginate conducting polymer. Therefore concluded that the conductivity would only determine the speed of the electrons during the regeneration. Nonetheless the efficiency of the regeneration process could be determined by the compatibility analysis of the conducting polymer and fluorophore. The compatibility analysis was carried out based on the energy level alignment between the E^o of the conducting polymer, and the HOMO energy level of the fluorophore. The calculated E^o of the conducting polymer used i.e., CMC/PVA is −3.144 eV, and alginate is −1.908 eV; incompatible to be paired with the fluorophore (PbS), which the HOMO, and LUMO energy levels are −5.100 eV, and −4.000 eV respectively. The low η of the CMC/PVA, and alginate-based cells however is speculated could also due to energy loss which is equivalent to 1.956 eV, and 3.912 eV energy offset respectively.

Selection and peer-review under responsibility of 4th Advanced Materials Conference 2018, 4th AMC 2018, 27th & 28th November 2018, Hilton Kuching Hotel, Kuching, Sarawak, Malaysia.

1. Introduction

Electron regeneration in the HOMO of fluorophore is a crucial process which completes the cycle of electron flow during a photovoltaic mechanism. A device structure and an ideal photovoltaic mechanism in a typical excitonic solar cell is illustrated in Fig. 1. The device consists of three main components which the function is stated in the parentheses i.e., (i) fluorophore (electron excitation), (ii) photoelectrode (electron transportation), and (iii) conducting polymer (electron regeneration). The fluorophore acts as a reactor for electron excitation upon absorption of photon with sufficient energy (E_{photon} > bandgap, $E_{g\text{-}fluorophore}$). The jump of an electron from the $HOMO_{fluorophore}$ to the $LUMO_{fluorophore}$ could be

* Corresponding author.
E-mail address: saifful@ump.edu.my (S.K. Muzakir).

https://doi.org/10.1016/j.matpr.2020.05.530
2214-7853/
Selection and peer-review under responsibility of 4th Advanced Materials Conference 2018, 4th AMC 2018, 27th & 28th November 2018, Hilton Kuching Hotel, Kuching, Sarawak, Malaysia.

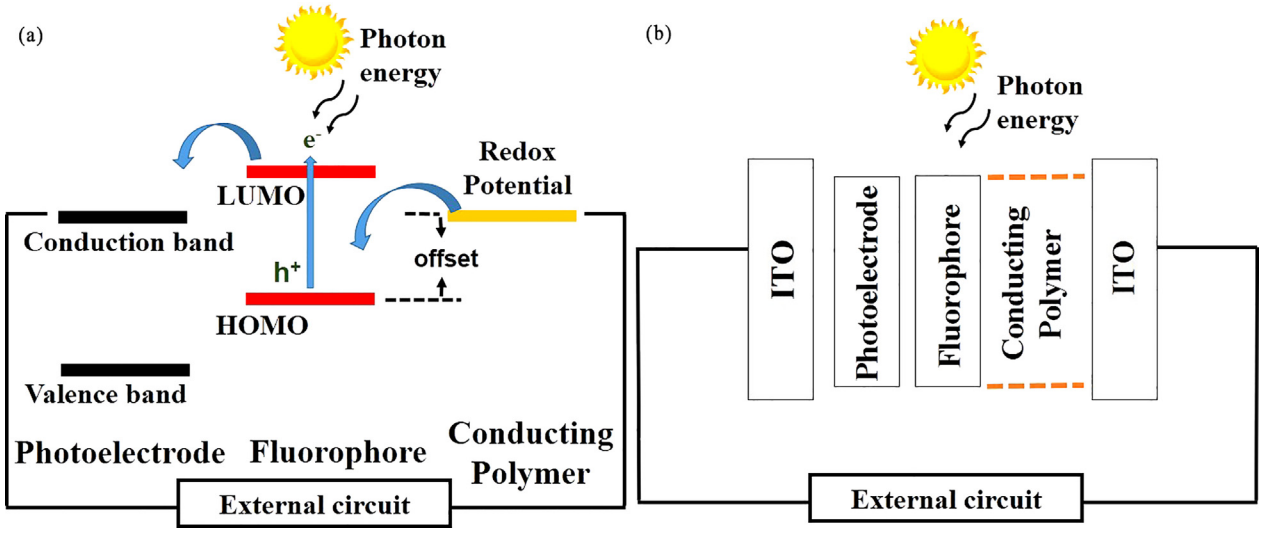

Fig. 1. (a) A device structure, and (b) working principle of an excitonic solar cell.

used as an analogy of the excitation, therefore leaving a vacancy (hole) in the $HOMO_{fluorophore}$. The photoelectrode (typical example e.g., metal oxide semiconductors) functions as a medium for transportation of the excited state electron from the fluorophore to the external circuit. The electron vacancy in the $HOMO_{fluorophore}$ could be replenished from the third process (electron regeneration) by the conducting polymer. Redox potential is the key that partially influences the efficiency of the regeneration. The conducting polymer would receive electron from the external circuit (reduction), and regenerate electron in the $HOMO_{fluorophore}$ (oxidation). Redox potential, E^o of the conducting polymer plays important role that determines the compatibility of the conducting polymer-fluorophore pair (which the $LUMO_{fluorophore} > E^o > HOMO_{fluorophore}$).

Quantum chemical calculations under the density functional theory (DFT) framework could be employed to calculate the E^o [1] with high accuracy. A comparison between the theoretical calculations and experimental results of the E^o of Cu-protein complexes has been made by Yan et al. (2016), which yielded insignificant error and standard deviation [2].

The effective mass of electron, m_e^* is a unique property of material; could be calculated using similar procedure to that of the E^o, where the details are discussed elsewhere. The m_e^* is correlated with the speed of electron movement, υ_d during the regeneration process, and mobility as depicted in the following equations:

$$\upsilon_d = \frac{\hbar(3\eta\pi^2)^{1/3}}{m_e^*} \quad (1)$$

$$\mu = (e \times \tau)/m_e^* \quad (2)$$

where η is the concentration of electron, τ is time of relaxation between two electron scattering incidents in the conducting polymer, which originated from defect and impurity [3,4]. The electron mobility is related with conductivity of a material, which represented by equation:

$$\sigma = \eta \times e \times \mu \quad (3)$$

where σ is conductivity, and e is charge of electron [5]. Therefore, the σ could be used as reference that described the speed of electron movement during the redox process. The conducting polymers are used in the recent efforts of fabrication of solar cell due to advancements made from the perspective of their conductivity. The CMC/PVA, and alginate conducting polymer showed achievement of $\sigma \sim 9.12 \times 10^{-6}$ S/cm [6], and 1.97×10^{-4} S/cm [7] at room temperature respectively.

2. Materials and method

2.1. Materials

Lead (II) sulfide (Aldrich 99.9%), nitric acid (ACS reagent, 37%), titanium dioxide (R&M chemicals), absolute ethanol (Merck, 99.5%), carboxymethyl cellulose (CMC), polyvinyl alcohol (PVA) and alginate powder (Sigma Aldrich).

2.2. Sample preparation

Indium-doped tin oxide (ITO) glass was cut into 2.5 cm × 2.5 cm. The working electrode of solar cell was prepared using the following methods. Titanium dioxide paste was prepared by dissolving 1.5 g TiO_2 powder with 1 ml of concentrated nitric acid and 2 ml of ethanol. The photoelectrode layer (TiO_2 paste) was fabricated using stencil printing technique on an active area of 1 cm × 1 cm, and heated at 100 °C for 10 min. Lead sulphide (0.24 g) layer was fabricated on the TiO_2 layer using thermal evaporator (Magna Value TEV) in an environment with pressure, potential, and current of 1.5×10^{-3} Torr, 1.53 V and 65 A, respectively to obtain good adsorption of the fluorophore (PbS) on the photoelectrode. Two conducting polymers were prepared in this work. The CMC/PVA-based conducting polymer was made by dissolving 2.0 g of CMC/PVA in 100 ml of distilled water. The mixture was continuously stirred for ca. 24 h to form a homogenous solution. The alginate-based conducting polymer was prepared by dissolving 2.0 g alginate in 100 ml of distilled water using similar procedure. A complete working solar cell was assembled by sandwiching few drops of the conducting polymer in between a working electrode and a blank ITO.

2.3. Lead chalcogenide cluster modelling

A thin film of PbS was fabricated on a glass using thermal evaporator at similar environment stated above. The thin film was characterized using X-Ray Diffractometer (Rigaku Miniflex II) – which the data is shown elsewhere. A PbS nanocluster which consists of 148 atoms was modelled using Gaussview 5.0 software based on the crystallographic properties. The geometry (bond lengths, bond

Please cite this article as: N. F. Shaafi, S. B. Aziz, M. F. Z. Kadird et al., A study of electron regeneration efficiency in fluorophore, Materials Today: Proceedings, https://doi.org/10.1016/j.matpr.2020.05.530

angles, and dihedral angles) of the model was optimized to the lowest energy structure using quantum chemical calculations; carried out using Gaussian 09W [8] software package at b3lyp/lanl2dz level of theory. The model was evaluated and established as realistic using harmonic frequency calculations; showed positive frequencies. Any models which showed negative frequencies were discarded due to non-realistic vibration mode. Subsequently, the ground state (HOMO), and excited state (LUMO) energy levels were calculated using Time-Dependent Density Functional Theory (TD-DFT).

Electron regenerations from the conducting polymer to the PbS involve reduction and oxidation processes. To mimic the electron regenerations, few possible initial charged-models of the molecule of conducting polymer were taken into consideration i.e., neutral (A^0), negative (A^{-1}), and positively-charged (A^{+1}) molecules. The oxidation process of the conducting polymer is presented as the following equations:

$$[A]^0 \rightarrow [A]^{+1} + 1e^- \quad (4)$$

$$[A]^{-1} \rightarrow [A]^0 + 1e^- \quad (5)$$

$$[A]^{+1} \rightarrow [A]^{+2} + 1e^- \quad (6)$$

The conducting polymer also would receive electron from the external circuit. The reduction process of the conducting polymer is presented as the following equations:

$$[A]^0 + 1e^- \rightarrow [A]^{-1} \quad (7)$$

$$[A]^{-1} + 1e^- \rightarrow [A]^{-2} \quad (8)$$

$$[A]^{+1} + 1e^- \rightarrow [A]^0 \quad (9)$$

Similar procedure was used to evaluate and establish realistic models of the conducting polymer; resulted realistic models of $[A]^0$ and $[A]^{-1}$. Furthermore, the electron regeneration efficiency was studied using the models of oxidation only which involved electron transfer from the conducting polymer to the PbS; therefore equation (5) was used as reference model of the regeneration. The 1-electron redox potential were calculated based on Born-Haber cycle (Fig. 2).

Six parameters were utilized during the calculations of redox potential i.e., (i) electron attachment enthalpy in gas phase (E_{SCF} I $_{(gas)}$), (ii) free energy of electron attachment in gas phase (G I $_{(gas)}$), (iii) thermal correction to Gibbs energy in gas phase (G_{corr}), (iv) difference of solvation free energy (ΔG I $_{(solv)}$), (v) electron attachment entalphy in solvation phase (E_{SCF} I $_{(solv)}$), and (vi) free energy of electron attachment in solvation phase (G I $_{(solv)}$). The calculations which involve the negatively-charged model were executed using the following method. The E_{SCF} I $_{(gas)}$ and G_{corr} were respectively obtained from geometry optimization and harmonic frequency calculations. G I $_{(gas)}$ was calculated using:

$$GI_{(gas)} = E_{SCF}I_{(gas)} + G_{corr} \quad (10)$$

G I $_{(solv)}$ was calculated using:

$$GI_{(solv)} = E_{SCF}I_{(solv)} + G_{corr} \quad (11)$$

ΔG $_{(solv)}$ was calculated using:

$$\Delta G_{(solv)} = E_{SCF}I_{(solv)} - E_{SCF}I_{(gas)} \quad (12)$$

Similar method was used to calculate the parameters which involve the neutral-state model i.e., E_{SCF} II $_{(gas)}$, G_{corr}, E_{SCF} II $_{(solv)}$, G II $_{(gas)}$, G II $_{(solv)}$, and ΔG $_{(solv)}$ II. The difference of solvation free energy ($\Delta G_{ox\ (solv)}$) was calculated using the following formula:

$$\Delta G_{ox(solv)} = GII_{(solv)} - -GI_{(solv)} \quad (13)$$

The standard 1-electron redox potential (E^0) was calculated using equation:

$$E^0 = \frac{\Delta Gox(solv)}{-F} \quad (14)$$

where the Faraday constant (F) is 23.06 kcal/mol.v with given value of −2.013770507 V compared to that of standard hydrogen electrode (SHE) which equivalent to −2.42623 eV. The redox potential value could be converted using the standardized conversion factor:

$$0\ V\ vs\ SHE = -4.44\ eV\ vs\ vacuum \quad (15)$$

3. Results and discussion

3.1. Energy level alignment analysis

An ideal energy level alignment of components of an excitonic solar cells (e.g., conducting polymer, fluorophore, and photoelectrode) is presented in Fig. 1 (b); would favor the following processes i.e., (i) electron regeneration from conducting polymer to $HOMO_{PbS}$, and (ii) electron injection from $LUMO_{PbS}$ to conduction band of photoelectrode. Therefore an efficient working mechanism of a solar cell could be achieved.

Through the quantum chemical calculations, the energy levels of fluorophore, and photoelectrode and redox potential were calculated. Device structure and alignment of the fabricated cells using different conducting polymers are presented in Fig. 3 (a)-(b), and (c)-(d) respectively. Efficient electron injection is hypothesized for both devices based on the perfect alignment between the $LUMO_{PbS}$ (−4.0 eV) and conduction band of TiO_2 (−4.1 eV) [9,10]; which comply the requirement of $LUMO_{PbS}$ > conduction band of TiO_2 with minimal energy loss during the injection (0.1 eV) [11]. However, efficient electron regeneration from the conducting polymer to the $HOMO_{PbS}$ is hindered due to extremely high redox

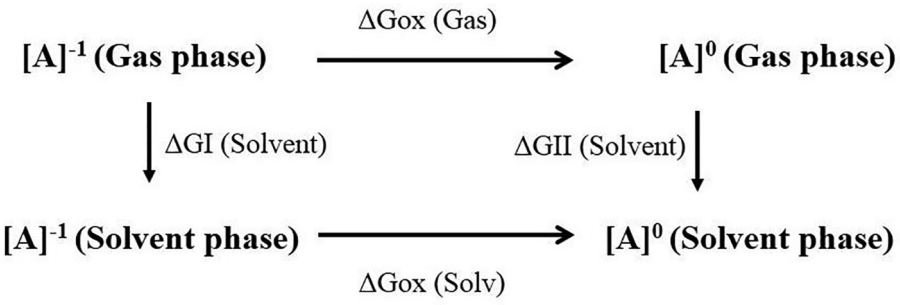

Fig. 2. Born-Haber cycle for standard redox potential calculations.

Please cite this article as: N. F. Shaafi, S. B. Aziz, M. F. Z. Kadird et al., A study of electron regeneration efficiency in fluorophore, Materials Today: Proceedings, https://doi.org/10.1016/j.matpr.2020.05.530

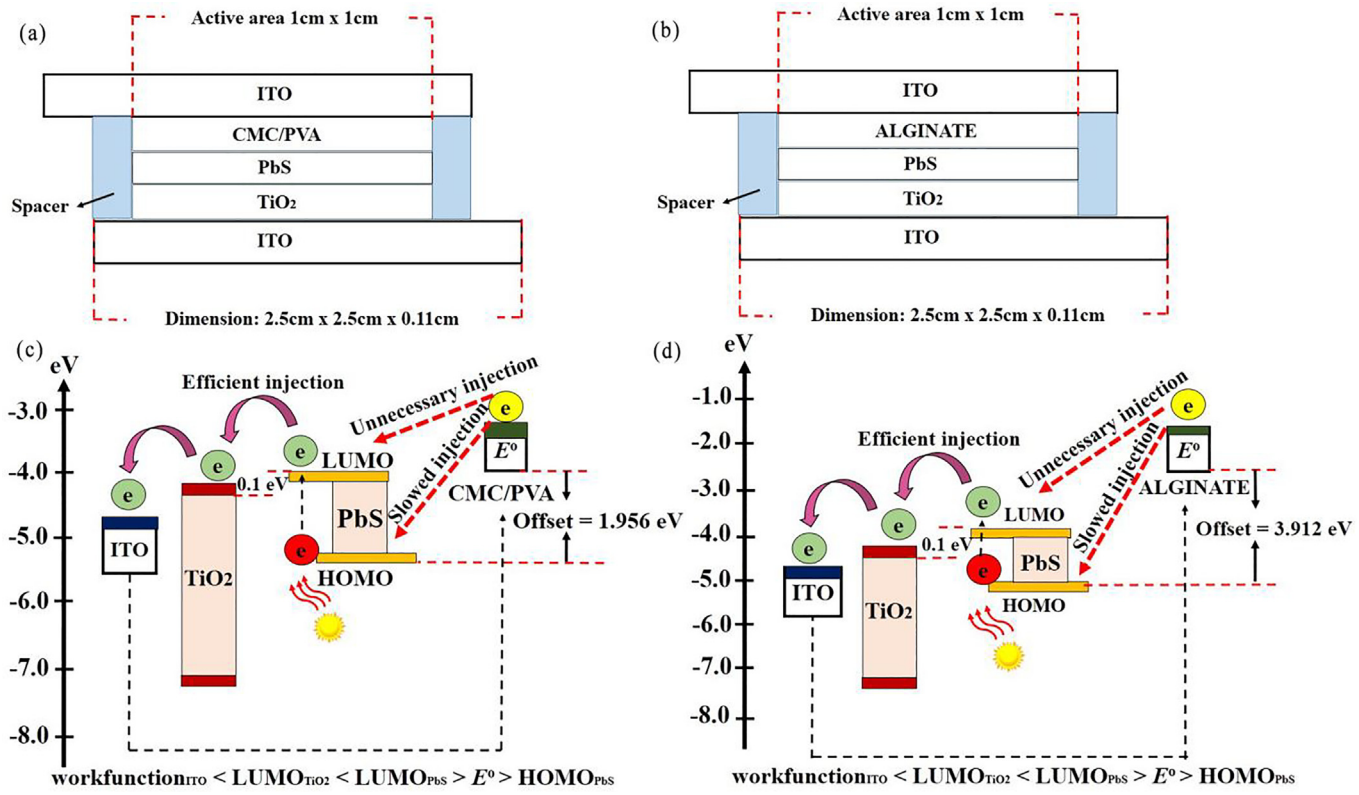

Fig. 3. Schematic diagram of the PbS-based cells using (a) CMC/PVA, (b) alginate conducting polymer, and energy level alignment of the fabricated cells with (c) CMC/PVA and (d) alginate conducting polymer.

potential i.e., $E^o_{alginate}$ (−1.908 eV) > $E^o_{CMC/PVA}$ (−3.144 eV) > $LUMO_{PbS}$ (−4.0 eV) > $HOMO_{PbS}$ (−5.1 eV).

The stated detrimental effect above was hypothesized due to two factors i.e., (i) unnecessary electron injection from conducting polymer to the $LUMO_{PbS}$, and (ii) slowed electron injection from conducting polymer to $HOMO_{PbS}$. The calculated E^o of the conducting polymer showed incompatible properties to be paired with the PbS; failed to fulfill the requirement of $LUMO_{PbS} > E^o > HOMO_{PbS}$.

3.2. Photovoltaic studies

In an ideal mechanism of photovoltaic, an electron would be excited from the $HOMO_{PbS}$ to $LUMO_{PbS}$ upon absorption of photon with sufficient energy ($E_{Photon} > Eg_{PbS}$). The excited state electron would undergo an injection mechanism from $LUMO_{PbS}$ to the conduction band of TiO_2; if the requirement of $LUMO_{PbS}$ > conduction band of TiO_2 is fulfilled. An ideal alignment of the PbS and TiO_2 are shown in the previous section, which favors an efficient electron injection from the PbS to TiO_2. Fig. 4 shows the efficiency of solar cells fabricated using CMC/PVA and alginate conducting polymer. The calculated photovoltaic parameters of the CMC/PVA-based i.e., photovoltaic conversion efficiency (η) = 0.0015%, open circuit voltage (V_{oc}) = 705 mV, short circuit current (I_{sc}) = 26 mA/m^2, maximum power (P_{max}) = 15 W/m^2, and fill factor (FF) = 82% under the condition of one Sun.

However, the calculated photovoltaic parameters for the alginate-based cell are inferior to the former cell; presented in Fig. 4 (b). During the excitation, a vacancy (hole) is created in the $HOMO_{PbS}$, therefore needs to be replenished via regeneration mechanism [12]. However, due to energy level misalignment between the E^o and $HOMO_{PbS}$, an efficient electron regeneration is hindered; therefore low η is yielded [13].

Furthermore, large offset of energy between the E^o and $HOMO_{PbS}$ is observed in Fig. 3 (c) - (d), i.e., $offset_{CMC/PVA\text{-}PbS}$ (1.956 eV), and $offset_{alginate\text{-}PbS}$ (3.912 eV) would favor unnecessary electron injection from the conducting polymer to the $LUMO_{PbS}$. Therefore, the yielded η for cellulose-based and alginate-based solar cells is 0.0015% and 0.00002% respectively. The misalignment nonetheless would suppress the electron regeneration from conducting polymer to the $HOMO_{PbS}$ [14]. The yielded photovoltaic parameters that support the findings of energy level analysis in the previous section, which correlated to the energy level misalignment between the conducting polymer and the PbS.

The CMC, PVA, and their composites are used in various applications e.g., photostability enhancement of dye-sensitized solar cell (DSSC) [15], as anode in the lithium ion batteries [16], and prevention of water penetration in electrical devices [17]. The CMC/PVA, and the alginate conducting polymer consists of three, and one carboxyl group respectively (Fig. 5). The high number of carboxyl functional group with co-existence of cation (Na^+ in both cases) would facilitate the regeneration of electron vacancy in the $HOMO_{PbS}$. Fast electron regeneration would lead to an efficient mechanism of electron excitation in the subsequent cycle; therefore, would yield high I_{sc} [18]. We have observed that the generated I_{sc} in the CMC/PVA is higher (26 mA/m^2) than that of the alginate-based

(2.46 mA/m^2) cell [19].

The conducting polymer of CMC and PVA have the ability to form hydrogen bonds due to the existence of characteristic functional group carboxylate anion ($-COO^-$) and hydroxyl (OH^-). According to S. Rudzhiah et al. (2015), the formation of hydrogen bonding could be induced and increase the ionic conductivity [20]. The blending method between CMC and PVA was believed to improve the ionic conductivity properties of conducting polymers by altering the structural behavior [6]. The CMC contains

Please cite this article as: N. F. Shaafi, S. B. Aziz, M. F. Z. Kadird et al., A study of electron regeneration efficiency in fluorophore, Materials Today: Proceedings, https://doi.org/10.1016/j.matpr.2020.05.530

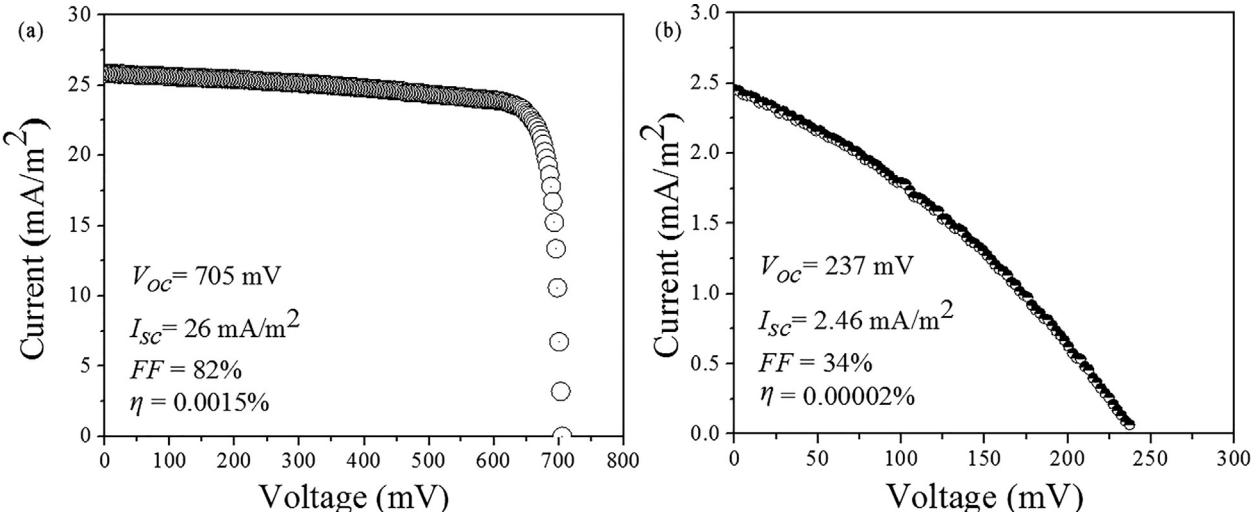

Fig 4. I-V curve of the photovoltaic parameters for fabricated lead sulphide-based thin film using (a) CMC/PVA and (b) alginate.

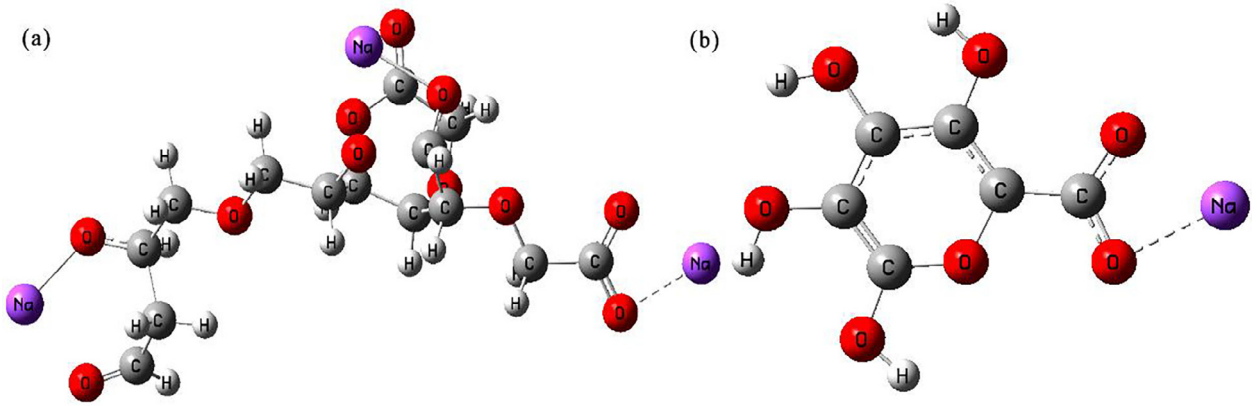

Fig. 5. Optimized structure of (a) CMC/PVA with composition 60:40 ratio and (b) alginate.

absence of dominant ion due to anionic polysaccharide properties of CMC, however the conductivity could be triggered by the motion of the conducting polymer chain which increases its flexibility upon addition of PVA [21]. The discussion on significant contribution of the CMC/PVA to the redox reaction is progressively debatable, however the presence of the redox reaction in the CMC/PVA conjugate could be proven upon expansion and contraction of bond lengths of the components [22]. The changes in bond length of CMC/PVA with oxidation number of 0 and −1 is shown in Table 1 upon simulation of oxidation potential. According to L. Bay et al. (2001), the changes in bond lengths and conformation in the conducting polymer could yield an intrinsic expansion. The changes of conducting polymer backbone on reduction/ oxidation could be induced by the expansion/ contraction effect; resulting from the osmotic effect, which yielded by the changes in the number of free ions in the CMC/PVA conducting polymer. Similar trend is observed in alginate conducting polymer with the oxidation number 0 and −1 which showed bond lengths i.e., (i) 0.09808537 nm, 0.09796263 nm (minimum), (ii) 0.24432798 nm, 0.23539426 nm (maximum), and (iii) 0.136182436 nm, 0.135576676 nm (average) respectively.

Table 1
Average, minimum and maximum bond length of CMC/PVA with different oxidation number.

Oxidation number	Average CMC/PVA bond length (nm)	Min CMC/PVA bond length (nm)	Max CMC/PVA bond length (nm)
0	0.14014	0.10918	0.25656
−1	0.14047	0.10917	0.25660

4. Conclusion

The redox potential of the CMC/PVA, and alginate-based conducting polymer are incompatible with the energy levels of PbS i.e., E^o > $LUMO_{PbS}$ > $HOMO_{PbS}$; therefore resulted inefficient electron regeneration. The E^o is higher than that of the $LUMO_{PbS}$, would favor unnecessary electron injection from the conducting polymer to the $LUMO_{PbS}$. Furthermore, the energy offset between the E^o and $HOMO_{PbS}$ is extremely large that would cause high energy loss during the electron regeneration i.e., $offset_{CMC/PVA\text{-}PbS}$ = 1.956 eV, and $offset_{alginate\text{-}PbS}$ = 3.912 eV. The unnecessary injection, and large offset therefore would hinder efficient electron regeneration in the $HOMO_{PbS}$. The fabricated cells using CMC/PVA, and alginate-based conducting polymer only showed 0.0015% and 0.00002% of photovoltaic conversion efficiency respectively due to the stated factors above. The device which utilized the CMC/PVA-based conducting polymer however showed high fill factor (82%), could be due to good adsorption of PbS onto the surface of TiO_2 with minimal effect of the conducting polymer.

Please cite this article as: N. F. Shaafi, S. B. Aziz, M. F. Z. Kadird et al., A study of electron regeneration efficiency in fluorophore, Materials Today: Proceedings, https://doi.org/10.1016/j.matpr.2020.05.530

Acknowledgements

This work if funded by the Research & Innovation Department of Universiti Malaysia Pahang, and the Ministry of Education of Malaysia through the Fundamental Research Grant Scheme (RDU 150111).

References

[1] S.Y. Lee, Bull. Korean Chem. Soc. 36 (2015) 443–444.
[2] L. Yan, Y. Lu, X. Li, Phys. Chem. Chem. Phys. 18 (2016) 5529–5536.
[3] K.I. Bolotin, K.J. Sikes, Z. Jiang, M. Klima, G. Fudenberg, J. Hone, P. Kim, H.L. Stormer, Solid State Commun. 146 (2008) 351–355.
[4] J. Wang, R. Zhao, M. Yang, Z. Liu, Z. Liu, J. Chem. Phys. 138 (2013) 084701.
[5] H.K. Kodali, B. Ganapathysubramanian, Sol. Energy Mater. Sol. Cells 111 (2013) 66–73.
[6] M.A. Saadiah, A.S. Samsudin, IOP Conf. Series Mater. Sci. Eng. 342 (2017) 012045.
[7] I. Caldeira, A. Lüdtke, F. Tavares, C. Cholant, R. Balboni, W.H. Flores, C.O. Avellaneda, Ionics 24 (2018) 413–420.
[8] J. Li, L.C. Xu, J.C. Chen, K.C. Zheng, L.N. Ji, J. Phys. Chem. A (2006) 8174–8180.
[9] T. Ju, R.L. Graham, G. Zhai, Y.W. Rodriguez, A.J. Breeze, L. Yang, S.A. Carter, Appl. Phys. Lett. 97 (2010) 43–106.
[10] M. Shalom, S. Ruhle, I. Hod, S. Yahav, A. Zaban, J. Am. Chem. Soc. 6 (2009) 9876–9877.
[11] B.E. Hardin, H.J. Snaith, M.D. McGehee, Nat. Photonics 6 (2012) 162–169.
[12] J. Bisquert, F. Fabregat-Santiago, I. Mora-Sero, G. Garcia-Belmonte, S. Gimenez, J. Phys. Chem. C 113 (2009) 17278–17290.
[13] S.K. Muzakir, Material Properties-Short Circuit Current Correlations in Quantum Dot Solar Cell, in Malaysia University Conference Engineering Technology (2014).
[14] M. Shalom, S. Ruhle, I. Hod, S. Yahav, A. Zaban, J. Am. Chem. Soc. 131 (2009) 9876–9877.
[15] S.K. Muzakir, N. Alias, M.M. Yusoff, Jose, Phys. Chem. Chem. Phys. 15 (2013) 16275–16285.
[16] R. Singh, A.R. Polu, B. Bhattacharya, H.W. Rhee, C. Varlikli, P.K. Singh, Sust. Energ. Rev. 65 (2016) 1098–1117.
[17] K. Das, D. Ray, N.R. Bandyopadhyay, A. Gupta, S. Sengupta, S. Sahoo, M. Misra, Ind. Eng. Chem. Res. 49 (2010) 2176–2185.
[18] M. Ziółek, C. Martín, L. Sun, A. Douhal, J. Phys. Chem. C 116 (2012) 26227–26238.
[19] S.A. Haque, E. Palomares, B.M. Cho, A.N. Green, N. Hirata, D.R. Klug, J.R. Durrant, J. Am. Chem. Soc. 127 (2005) 3456–3462.
[20] S. Rudhziah, A. Ahmad, I. Ahmad, N.S. Mohamed, Electrochim. Acta 175 (2015) 162–168.
[21] A.S. Samsudin, M.A, J. Non-Cryst. Solids 497, (2018) 19-29.
[22] L. Bay, T. Jacobsen, S. Skaarup, K. West, J. Phys. Chem. B 105 (36) (2001) 8492–8497.

Further Reading

[1] J. Wang, J. Hu, X. Sun, A.M. Agarwal, L.C. Kimerling, D.R. Lim, R.A. Synowicki, J. Appl. Phys. 104 (2008) 053707.
[2] R.S. Kane, R.E. Cohen, R. Silbey, J. Phys. Chem. 100 (1996) 7928–7932.
[3] A.L. Rogach, A. Eychmüller, S.G. Hickey, S.V. Kershaw, Small 3 (2007) 536–557.

Please cite this article as: N. F. Shaafi, S. B. Aziz, M. F. Z. Kadird et al., A study of electron regeneration efficiency in fluorophore, Materials Today: Proceedings, https://doi.org/10.1016/j.matpr.2020.05.530